AIP | Applied Physics Letters

Atomic layer deposition of HfO2 on graphene through controlled ion beam treatment

Ki Seok Kim, Il-Kwon Oh, Hanearl Jung, Hyungjun Kim, Geun Young Yeom, and Kyong Nam Kim

Citation: Applied Physics Letters **108**, 213102 (2016); doi: 10.1063/1.4950997
View online: http://dx.doi.org/10.1063/1.4950997
View Table of Contents: http://scitation.aip.org/content/aip/journal/apl/108/21?ver=pdfcov
Published by the AIP Publishing

Atomic layer deposition of HfO_2 on graphene through controlled ion beam treatment

Ki Seok Kim,[1] Il-Kwon Oh,[2] Hanearl Jung,[2] Hyungjun Kim,[2] Geun Young Yeom,[1,3,a)] and Kyong Nam Kim[4,a)]
[1]*School of Advanced Materials Science and Engineering, Sungkyunkwan University, 2066 Seobu-ro, Jangan-gu, Suwon-si, Gyeonggi-do 16419, South Korea*
[2]*School of Electrical and Electronics Engineering, Yonsei University, 50 Yonsei Ro, Seodaemun-gu, Seoul 120-749, South Korea*
[3]*SKKU Advanced Institute of Nano Technology (SAINT), Sungkyunkwan University, 2066 Seobu-ro, Jangan-gu, Suwon-si, Gyeonggi-do 16419, South Korea*
[4]*School of Advanced Materials Science and Engineering, Daejeon University, Yongun-dong, Dong-gu, Daejeon 34520, South Korea*

(Received 7 March 2016; accepted 9 May 2016; published online 23 May 2016)

The polymer residue generated during the graphene transfer process to the substrate tends to cause problems (e.g., a decrease in electron mobility, unwanted doping, and non-uniform deposition of the dielectric material). In this study, by using a controllable low-energy Ar^+ ion beam, we cleaned the polymer residue without damaging the graphene network. HfO_2 grown by atomic layer deposition on graphene cleaned using an Ar^+ ion beam showed a dense uniform structure, whereas that grown on the transferred graphene (before Ar^+ ion cleaning) showed a non-uniform structure. A graphene–HfO_2–metal capacitor fabricated by growing 20-nm thick HfO_2 on graphene exhibited a very low leakage current ($<10^{-11}$ A/cm^2) for Ar^+ ion-cleaned graphene, whereas a similar capacitor grown using the transferred graphene showed high leakage current. *Published by AIP Publishing.*
[http://dx.doi.org/10.1063/1.4950997]

Graphene has extraordinary properties, such as high electron mobility, in addition to excellent mechanical strength and high thermal conductivity.[1–4] Due to the high electron mobility of graphene, logic devices using graphene possess remarkable properties, among which include proposed beyond complementary metal oxide semiconductor (CMOS) nanoelectronics.[5–8]

Currently, for large-area graphene electronics, graphene grown on Cu foils by chemical vapor deposition requires transfer to the substrate and lithographic patterning. For that reason, the polymer layer, such as that of poly(methyl methacrylate) (PMMA),[9] must be removed after the graphene transfer to the substrate[9–11] and lithographic patterning.[12–15] However, a very thin polymer residue remains on the graphene surface after the polymer layer removal, and this residue can cause many problems, such as decreased electron mobility[16] and the prevention of uniform coverage of high-*k* dielectrics or metals on graphene during atomic layer deposition (ALD) through prevention of precursor absorption on the graphene surface.[17,18]

With regard to high-*k* ALD on graphene, researchers initially believed that the difficulty in forming a high-*k* dielectric on the transferred graphene surface originated from the chemical stability of the graphene surface, due to the sp^2 bonding of its honeycomb structure.[19] Therefore, to deposit a high-*k* dielectric layer on graphene by ALD, researchers deposit a buffer layer and a seed layer before performing high-*k* ALD on the graphene surface.[19–27] Alternatively, to directly deposit high-*k* dielectric materials by ALD on the transferred graphene without depositing a seed layer, researchers treat the graphene surface with nitrogen plasma and oxygen plasma,[28,29] or increase the reactivity of the graphene surface by ozone adsorption.[30,31] In fact, we believe that the difficulty in depositing high-*k* dielectric materials on the graphene surface by ALD appears more due to the polymer residue on the transferred graphene surface after the transfer to the substrate or lithographic patterning.

In this paper, we used a monoenergetic Ar^+ ion beam with an energy of less than ~10 eV for removal of the residue on the graphene surface. By removing the residue, we accomplished in fabricating a graphene–HfO_2–metal capacitor, comparing the characteristics of leakage current.

We synthesized monolayer graphene on a Cu foil by a CVD method. We preheated Cu foil (electroplated Cu film; 99.9(%); purchased from Wacopa) at 1020 °C with Ar (1000 sccm) and H_2 (100 sccm) gases for 30 min to reduce the surface roughness. Then, we flew CH_4 (5 sccm) into the chamber with Ar (1000 sccm) and H_2 (20 sccm) for 20 min at 1020 °C to grow graphene on the Cu foil; thereafter, we flew Ar (1000 sccm) to cool down the reactor to room temperature. After graphene synthesis, we cut the Cu foil into pieces, coating with PMMA (Microchem 950C), then immersing into a $FeCl_3$ solution in order to etch away the Cu foil. When the Cu foil was completely removed, we rinsed the graphene layer on PMMA in deionized water to wash away etchant residues. Then, we transferred the PMMA-coated graphene layer onto the Si wafer with a 300-nm thick SiO_2 layer. We removed the PMMA on the SiO_2/Si wafer using acetone after completely adhering the graphene onto the wafer.

We exposed the graphene on SiO_2 to a low-energy Ar^+ ion beam, using a 4-in. diameter two-grid Ar^+ ion beam

a)Authors to whom correspondence should be addressed. Electronic addresses: knam1004@dju.kr and gyyeom@skku.edu

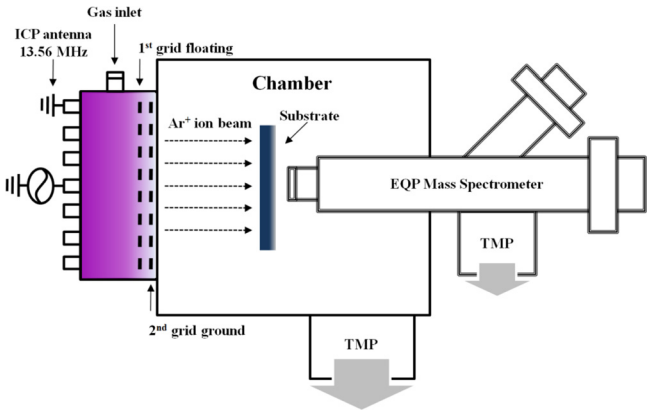

FIG. 1. Schematic diagram of a two-grid Ar^+ ion beam treatment system. To measure the Ar^+ ion energy distribution, we installed a mass spectrometer at the substrate location. We loaded substrate through a load-lock system.

system, investigating the effect of the Ar^+ ion beam on the change in plasma condition (Fig. 1) [Plasma condition: base pressure: 3×10^{-6} Torr; Ar gas flow rate: 200 sccm and 240 sccm; ICP power: 500 W; 1st grid voltage: floated; 2nd grid voltage: grounded]. The Ar^+ ion beam consisted of an ICP source (13.56 MHz) and two grids in front of the ICP source to extract and control the energy of the Ar^+ ions. We installed the mass spectrometer at the substrate location; therefore, we could measure the exact Ar^+ ion energy distribution.

We deposited HfO_2 by ALD on the graphene surface transferred onto the Si wafer with a 300-nm thick SiO_2 layer (precursor: TDMAHf; reactant: H_2O; $T_{(substrate)}$: 200 °C) by using an ALD apparatus. To fabricate a metal–insulator–metal (MIM) capacitor, we deposited a 20-nm thick HfO_2 layer on the transferred graphene surface and on the graphene surface cleaned using the Ar^+ ion beam. We removed a portion of the HfO_2 layer using an HF solution (HF:deionized water = 1:200) to expose the graphene, and we deposited an Au (50 nm)/Cr (5 nm) layer on the HfO_2 and graphene to form a MIM capacitor.

We observed the surface morphology of the cleaned graphene and HfO_2 deposited on the graphene surface using field-emission scanning electron microscopy (FESEM, S-4700, Hitachi). We examined the graphene surface cleaning by Raman spectroscopy (WITEC Alpha 300M$^+$ 532-nm wavelength). We measured the thickness of HfO_2 deposited by ALD using an ultraviolet-visible (UV-Vis) spectroscopic ellipsometer (SE MG-1000UV, NANO-VIEW) at a tilt angle of 70°. We observed atomic images of the graphene surface using high-resolution transmission electron microscopy (HR-TEM, Titan G2 Cube Cs-corrected, FEI) at 80 kV. We measured the leakage current in the MIM capacitor using a semiconductor parameter analyzer (4145b, HP) at low biases (<2 V).

As shown in Figs. 2(a) and 2(b), we could measure the energy of the Ar^+ ion beam for a fixed 500 W of rf power, according to the Ar flow rate. As shown in the figures, the energy of the Ar^+ ions beam showed a Gaussian-shaped energy distribution peak at about 9.5 eV and about 13.4 eV for 240 sccm and 200 sccm of Ar flow rate, respectively. Figs. 2(c) and 2(d) show the Raman spectroscopic data for the graphene exposed at 9.5 eV and 13.4 eV for 300 s. As shown in Fig. 2(c), no change in D peak intensity at ~1335 cm^{-1}, indicating no additional damage to the graphene surface by the Ar^+ ion exposure at 9.5 eV. As shown in Fig. 2(d), with increasing Ar^+ ion beam energy, the D peak intensity increased, indicating increased defect formation on the graphene surface. However, upon exposure to the 9.5 eV Ar^+ ion beam for 300 s, the positions of the G and 2D peaks blue-shifted to higher frequencies by about ~16 cm^{-1} and ~15 cm^{-1}, respectively, whereas the D peak position did not change. One generally observes a blue shift of Raman G/2D peaks when removing a p-type doping material from the graphene surface.[32] Therefore, we can attribute the peak shifts caused by the Ar^+ ion cleaning and indicated by Raman spectroscopic data in Fig. 2(c) to the removal of the PMMA residue on the graphene surface.

We observed the graphene surface before and after Ar^+ ion cleaning using high-resolution transmission electron

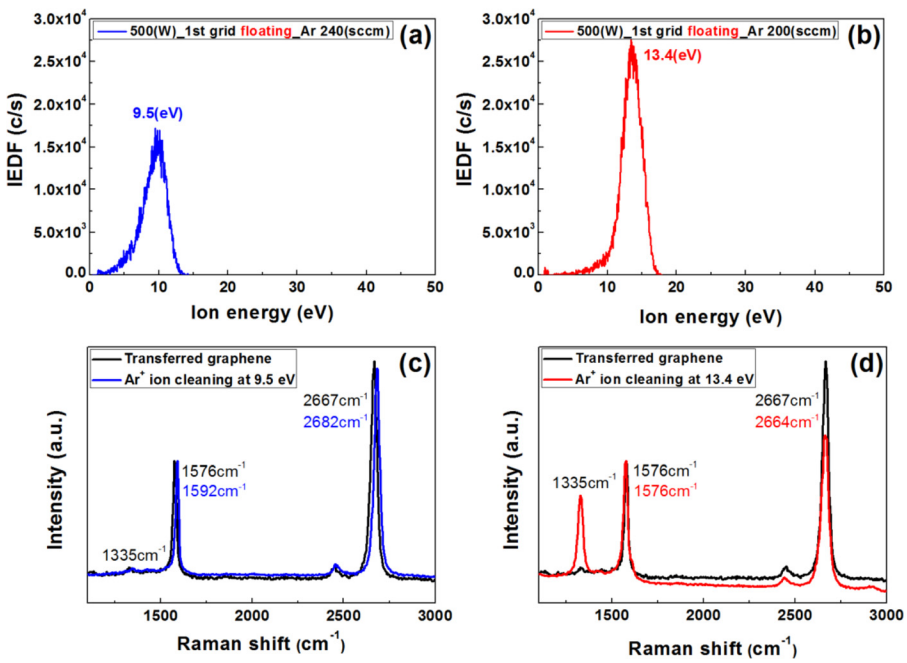

FIG. 2. Ar^+ ion energy distribution of the Ar^+ ion source for different Ar gas flow rates at: (a) 240 sccm and (b) 200 sccm. Raman spectroscopic data for the graphene surface after Ar^+ ion beam treatments for 300 s at: (c) 9.5 eV and (d) 13.4 eV.

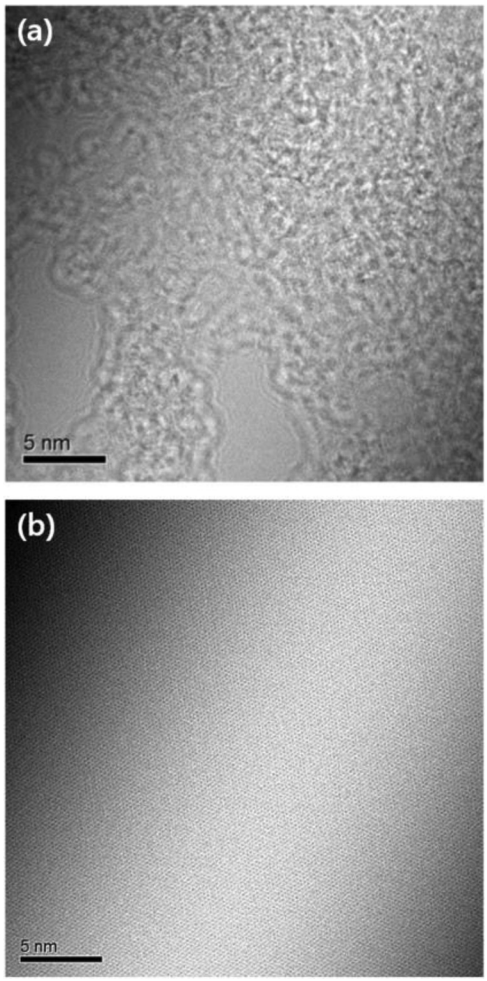

FIG. 3. HR-TEM images of monolayer graphene: (a) transferred graphene before Ar^+ ion cleaning and (b) after Ar^+ ion cleaning for 300 s.

microscopy (HR-TEM), with the results shown in Figs. 3(a) for the transferred graphene and 3(b) for 300 s cleaning. As shown in Fig. 3(a), we obtained a hazy atomic image, owing to the PMMA residue on the graphene surface. However, as shown in Fig. 3(b), we could observe a very clean graphene atomic image after the Ar^+ ion cleaning for 300 s, indicating effective graphene surface cleaning using the Ar^+ ion cleaning method. We also took scanning electron microscope (SEM) images of the graphene surface after the transfer to the SiO_2 substrate using PMMA and those after the low-energy Ar^+ ion cleaning (see supplementary material Fig. S1[33]). In fact, for the graphene surface cleaning, other methods (e.g., surface cleaning using H_2 and H_2-N_2 plasmas,[34] and CO_2 cluster[35]) also exhibited a clean graphene surface after the cleaning. However, in such research, possible damages that could form on the surface during the cleaning process have not been explicitly described, and these methods could also result in unintentional doping during the processing. Contrariwise, in our method using a 9.5 eV monoenergetic Ar^+ ion beam, as shown in Fig. 3(b), we could remove the PMMA residue without forming surface damage and without unintentional doping on the surface. In addition, when we fabricated a back-gate graphene field effect transistor (FET) in a previous research,[36] not only the charge neutrality point (Dirac point) of the FET fabricated after the graphene cleaning shifted to near 0 V, but also the drain current of the FET increased about four times.

On transferred and Ar^+ ion-cleaned graphene surfaces, we deposited a 20-nm thick HfO_2 layer by ALD, investigating the deposition behavior of the HfO_2. As a reference, we also deposited HfO_2 on a fresh graphene surface grown on a Cu foil (before transfer to a SiO_2 substrate) and on the SiO_2 substrate itself. Fig. 4 shows the SEM images of the HfO_2 deposited on: the graphene on Cu (Fig. 4(a)); the graphene after transfer to the SiO_2 (with PMMA residue still present on the surface after PMMA removal by acetone, after transfer to the SiO_2 from the Cu foil) (Fig. 4(b)); the graphene after removal of the PMMA residue by the 9.5 eV Ar^+ ion beam (Fig. 4(c)); and the SiO_2 surface (with no graphene on the surface) (Fig. 4(d)). As shown in Fig. 4(b), we observed non-uniform HfO_2 growth for transferred graphene, possibly owing to the PMMA residue on the surface; whereas we observed very uniform HfO_2 growth on the graphene surface after the Ar^+ ion cleaning, as shown in

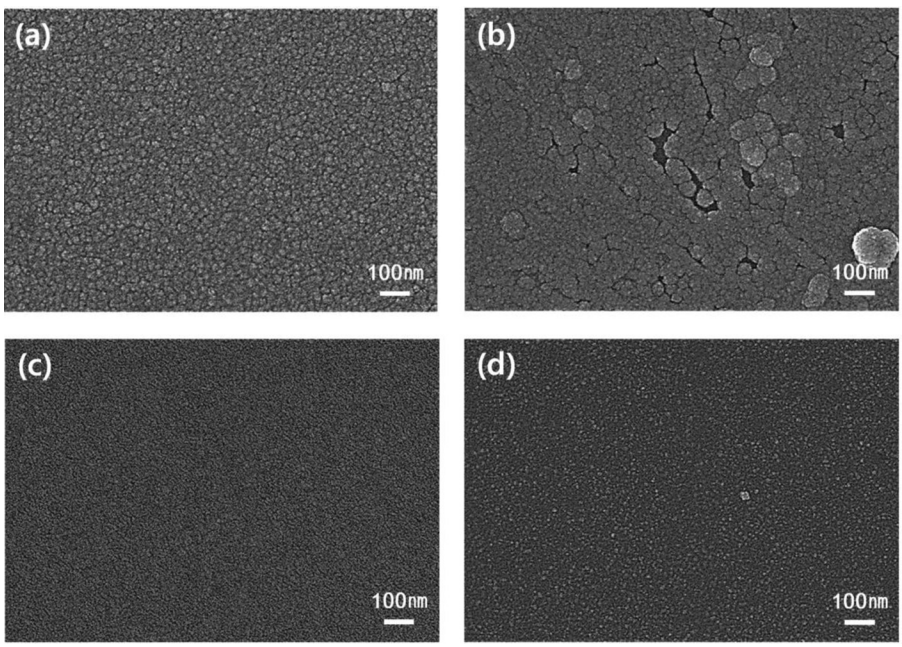

FIG. 4. SEM images of 20-nm thick HfO_2 layer deposited by ALD on: (a) the graphene surface on Cu foil (just after graphene growth on Cu by CVD); (b) the graphene after transfer to the SiO_2 surface (with PMMA used to transfer graphene removed by acetone, and PMMA residue still present on the graphene surface); (c) the graphene cleaned using an Ar^+ ion beam; and (d) the SiO_2 surface (with no graphene on the surface).

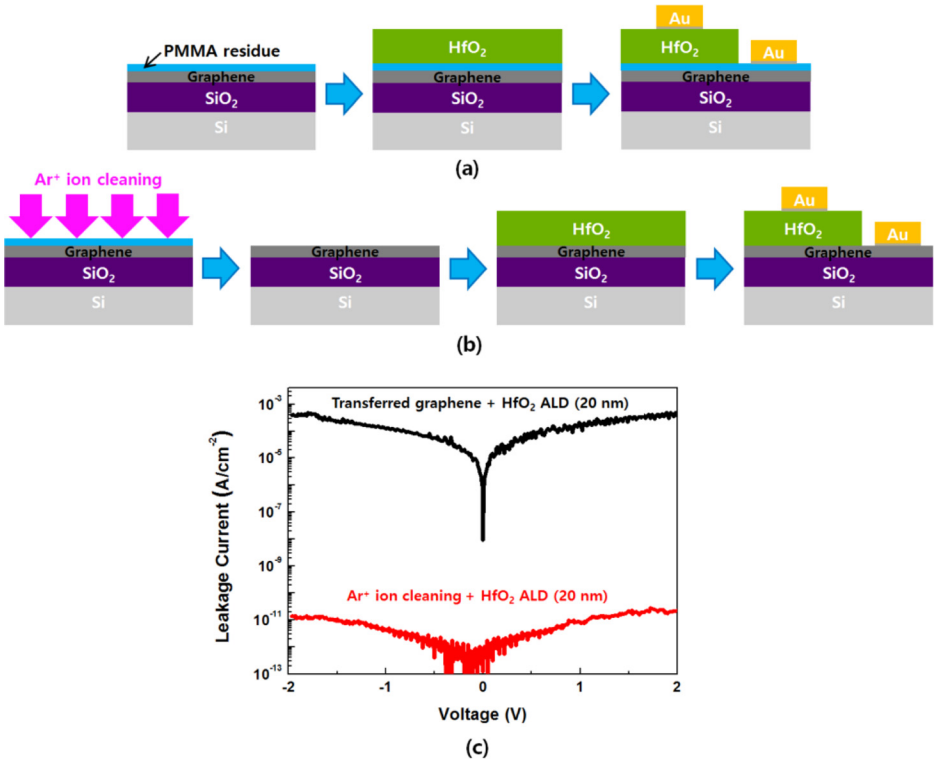

FIG. 5. Schematic showing the fabrication sequence of HfO_2 capacitors by ALD on graphene: (a) without cleaning and (b) with cleaning. (c) Leakage currents in capacitors fabricated using HfO_2 grown on the transferred graphene (black) and on graphene cleaned using an Ar^+ ion beam (red).

Fig. 4(c). The HfO_2 thin films grown on fresh graphene on the Cu foil and SiO_2 in Figs. 4(a) and 4(d), respectively, also showed uniform HfO_2 growth, indicating that the non-uniform growth of HfO_2 on the transferred graphene was due to the PMMA residue on the graphene surface after the transfer from Cu to SiO_2 (obstructing the growth of HfO_2 on the graphene surface).

We compared the qualities of HfO_2 grown on the graphene surface before and after the Ar^+ ion cleaning by fabricating capacitors using HfO_2 grown on the graphene surface, as shown in Figs. 5(a) and 5(b), respectively. Fig. 5(c) shows leakage currents from the capacitors fabricated using a 20-nm thick HfO_2 layer grown on the transferred graphene (black) and graphene cleaned using the Ar^+ ion beam (red). Figs. 5(a) and 5(b) show the fabrication sequences for the HfO_2 capacitors. We deposited a 20-nm thick HfO_2 layer by ALD on the transferred graphene surface and on the graphene surface cleaned using the Ar^+ ion beam. On the transferred graphene surface, a thin PMMA residue was still present; therefore, a lower-quality HfO_2 layer formed on the transferred graphene surface. When we removed the thin PMMA residue using the Ar^+ ion beam, a higher-quality HfO_2 layer formed on the clean graphene surface. As shown in Fig. 5(c), the capacitor fabricated using a 20-nm thick HfO_2 layer grown on the transferred graphene showed significant leakage current, owing to the non-uniform growth of the HfO_2 on the transferred graphene surface. In contrast, the capacitor fabricated using graphene cleaned with the 9.5 eV Ar^+ ion beam showed a very low leakage current of less than 10^{-11} A/cm^2, owing to the dense HfO_2 thin film grown on the graphene surface. The schematic diagram of the graphene surface cleaning and the HfO_2 growth on the cleaned graphene surface is shown in supplementary material Fig. S2.[33]

In this study, we transferred graphene layers from a Cu foil by using PMMA, while the PMMA residue generated during the transfer process cannot be easily removed by wet cleaning techniques. By using a controllable low-energy Ar^+ ion beam (9.5 eV), we removed the PMMA residue on the graphene surface without damaging the graphene surface. The capacitor fabricated with the HfO_2 grown on the graphene surface cleaned by the Ar^+ ion beam exhibited a lower leakage current, owing to the denser HfO_2 layer.

This research was supported by the Industry Technology R&D program of MOTIE/KEIT [10050501, Development of a laser-assisted hybrid inorganic deposition system for flexible organic device passivation] and the Basic Science Research Program through the National Research Foundation of Korea (NRF), funded by the Ministry of Education (2015R1D1A4A01020731).

[1]K. S. Novoselov, A. K. Geim, S. V. Morozov, D. Jiang, Y. Zhang, S. V. Dubonos, I. V. Grigorieva, and A. A. Firsov, Science **306**, 666 (2004).
[2]K. S. Novoselov, A. K. Geim, S. V. Morozov, D. Jiang, M. K. I. Grigorieva, S. Dubonos, and A. Firsov, Nature **438**, 197 (2005).
[3]Y. Zhang, Y. Tan, H. L. Stormer, and P. Kim, Nature **438**, 201 (2005).
[4]A. A. Balandin, S. Ghosh, W. Bao, I. Calizo, D. Teweldebrhan, F. Miao, and C. N. Lau, Nano Lett. **8**, 902 (2008).
[5]V. V. Cheianov, V. Fal'ko, and B. L. Altshuler, Science **315**, 1252 (2007).
[6]S. K. Banerjee, L. F. Register, E. Tutuc, D. Basu, S. Kim, D. Reddy, and A. H. MacDonald, IEEE Proc. **98**, 2032 (2010).
[7]S. K. Banerjee, L. F. Register, E. Tutuc, D. Reddy, and A. H. MacDonald, IEEE Electron Device Lett. **30**, 158 (2009).
[8]S. Tanachutiwat, J. Ung Lee, W. Wang, and C. Y. Sung, Proceedings of the 2010 47th ACM/IEEE Conference, Anaheim, CA (IEEE, 2010), p. 883.
[9]X. Li, W. Cai, J. An, S. Kim, J. Nah, D. Yang, R. Piner, A. Velamakanni, I. Jung, E. Tutuc, S. K. Banerjee, L. Colombo, and R. S. Ruoff, Science **324**, 1312 (2009).
[10]X. Li, Y. Zhu, W. Cai, M. Borysiak, B. Han, D. Chen, R. D. Piner, L. Colombo, and R. S. Ruoff, Nano Lett. **9**, 4359 (2009).
[11]Z. Yan, J. Lin, Z. Peng, Z. Sun, Y. Zhu, L. Li, C. Xiang, E. L. Samuel, C. Kittrell, and J. M. Tour, ACS Nano **6**, 9110 (2012).
[12]M. Ishigami, J. Chen, W. Cullen, M. Fuhrer, and E. Williams, Nano Lett. **7**, 1643 (2007).
[13]L. A. Ponomarenko, F. Schedin, M. I. Katsnelson, R. Yang, E. W. Hill, K. S. Novoselov, and A. K. Geim, Science **320**, 356 (2008).

[14]Y. Lin, C. Lu, C. Yeh, C. Jin, K. Suenaga, and P. Chiu, Nano Lett. **12**, 414 (2012).
[15]Y. Lim, D. Lee, T. Shen, C. Ra, J. Choi, and W. J. Yoo, ACS Nano **6**, 4410 (2012).
[16]A. Pirkle, J. Chan, A. Venugopal, D. Hinojos, C. Magnuson, S. McDonnell, L. Colombo, E. Vogel, R. Ruoff, and R. Wallace, Appl. Phys. Lett. **99**, 122108 (2011).
[17]C. Wilson, R. Grubbs, and S. George, Chem. Mater. **17**, 5625 (2005).
[18]K. Kim, H. Lee, R. W. Johnson, J. T. Tanskanen, N. Liu, M. Kim, C. Pang, C. Ahn, S. F. Bent, and Z. Bao, Nat. Commun. **5**, 4781 (2014).
[19]X. Wang, S. M. Tabakman, and H. Dai, J. Am. Chem. Soc. **130**, 8152 (2008).
[20]D. B. Farmer and R. G. Gordon, Nano Lett. **6**, 699 (2006).
[21]J. R. Williams, L. Dicarlo, and C. M. Marcus, Science **317**, 638 (2007).
[22]Y. Lin, K. A. Jenkins, A. Valdes-Garcia, J. P. Small, D. B. Farmer, and P. Avouris, Nano Lett. **9**, 422 (2009).
[23]D. B. Farmer, H. Chiu, Y. Lin, K. A. Jenkins, F. Xia, and P. Avouris, Nano Lett. **9**, 4474 (2009).
[24]F. Xia, D. B. Farmer, Y. Lin, and P. Avouris, Nano Lett. **10**, 715 (2010).
[25]S. Kim, J. Nah, I. Jo, D. Shahrjerdi, L. Colombo, Z. Yao, E. Tutuc, and S. K. Banerjee, Appl. Phys. Lett. **94**, 062107 (2009).
[26]M. J. Hollander, M. LaBella, Z. R. Hughes, M. Zhu, K. A. Trumbull, R. Cavalero, D. W. Snyder, X. Wang, E. Hwang, and S. Datta, Nano Lett. **11**, 3601 (2011).
[27]V. K. Sangwan, D. Jariwala, S. A. Filippone, H. J. Karmel, J. E. Johns, J. M. Alaboson, T. J. Marks, L. J. Lauhon, and M. C. Hersam, Nano Lett. **13**, 1162 (2013).
[28]T. Lim, D. Kim, and S. Ju, Appl. Phys. Lett. **103**, 013107 (2013).
[29]O. M. Nayfeh, T. Marr, and M. Dubey, IEEE Electron Device Lett. **32**, 473 (2011).
[30]B. Lee, G. Mordi, M. J. Kim, Y. J. Chabal, E. M. Vogel, R. M. Wallace, K. J. Cho, L. Colombo, and J. Kim, Appl. Phys. Lett. **97**, 043107 (2010).
[31]S. Jandhyala, G. Mordi, B. Lee, G. Lee, C. Floresca, P. Cha, J. Ahn, R. M. Wallace, Y. J. Chabal, and M. J. Kim, ACS Nano **6**, 2722 (2012).
[32]H. Shin, W. M. Choi, D. Choi, G. H. Han, S. Yoon, H. Park, S. Kim, Y. W. Jin, S. Y. Lee, and J. M. Kim, J. Am. Chem. Soc. **132**, 15603 (2010).
[33]See supplementary material at http://dx.doi.org/10.1063/1.4950997 for additional information and experimental results.
[34]G. Cunge, D. Ferrah, C. Petit-Etienne, A. Davydova, H. Okuno, D. Kalita, V. Bouchiat, and O. Renault, J. Appl. Phys. **118**, 123302 (2015).
[35]S. Gahng, C. H. Ra, Y. J. Cho, J. A. Kim, T. Kim, and W. J. Yoo, Appl. Phys. Lett. **104**, 223110 (2014).
[36]K. S. Kim, H. Hong, H. Jung, I. Oh, Z. Lee, H. Kim, G. Y. Yeom, and K. N. Kim, Carbon **104**, 119 (2016).